ANELASTIC RELAXATION PHENOMENA IN ALUMINA-SPINEL REFRACTORIES

Ilona Kieliba*,Thorsten Tonnesen, Rainer Telle
Institute of Mineral Engineering, RWTH Aachen University, Germany

Marc Huger
IRCER - University of Limoges, Limoges, France

ABSTRACT

Due to the desired combination of properties like high melting point, excellent corrosion resistance to steel-making slag and superior thermal shock resistance spinel is increasingly incorporated into multiple refractory solutions. Despite the heavy focus on spinel in various fields of science and engineering as well as extensive research conducted, there is still little known about the stress relaxation ability of spinel containing materials. The objective of this work is to investigate the anelastic relaxation phenomena in various alumina – spinel refractories, to determine the underlying mechanism and assess their influence on thermomechanical properties.

1. INTRODUCTION

Similarly to the purely elastic behavior, the anelastic behavior is characterized by linearity and complete recoverability but in the contrary to elastic deformation, which is instantaneous, additional time-dependent deformation occurs. When a constant strain is imposed to an anelastic solid the stress is relaxed in time-dependent manner. The anelastic response is a manifestation of internal relaxation processes taking place in order to achieve a new equilibrium state. Such a system equilibration usually involves motion of some microstructural units such as point defects, dislocations or grain boundaries. Anelastic relaxation phenomena give rise to increased damping (internal friction) capacity, which represents the ability of the material to dissipate or absorb vibrational energy by microstructural features in the material.

The ability of the material to deform in anelastic manner and thus develop high damping capacity may have practical implications in service. This statement may be extremely relevant for materials working in high temperature environment, where multiple thermally activated relaxation processes can take place.

Although the phenomenon of anelastic strengthening is not very common, it has been shown that in the case of zirconia ceramics [1-2] the ability to deform in anelastic manner contributed to enhanced tensile fracture strength. Similarly, a direct correlation between increased internal friction capacity and enhanced critical stress intensity factor K_{IC} has been provided for the WC-Co composites [3]. Furthermore, the anelastic ability to relax thermal stresses by dislocation generation and motion instead of crack initiation, has been shown to improve the thermal fatigue resistance of high-damping magnesium matrix [4] and Al-Al_2O_3 [5] composites. On the other hand, as described in the literature [6], increased damping at high temperatures may correspond to the degradation of mechanical properties and increased creep rate.

The aim of the present research is to investigate the anelastic relaxation characteristic of various alumina-spinel refractories via damping temperature dependency determination. Obtained damping spectra have been correlated with Young's modulus, HMOR and creep properties. In addition, the hypothesis that high-damping materials may exhibit increased thermal shock resistance, has been proven based on both monolithic and shaped alumina-spinel refractory solutions.

2. EXPERIMENTAL PROCEDURE

2.1 **Materials**

Within this investigation, two main types of alumina-rich spinel containing refractories were tested namely alumina-spinel brick and a set of alumina-spinel castables.

Alumina-spinel brick is made up of coarser white fused alumina aggregates embedded in a fine matrix composed of alumina-rich spinel and alumina fines, with the total spinel content of 25 wt%.

Five model castables were prepared accordingly to the formulations presented in **Table I.** The raw materials: TA or WFA, CMA 72 or Secar 71 (Imerys, France), reactive alumina and calcined alumina (Alteo, France), spinel AR78 <20µm and <45µm (Almatis, Germany) and fluidifier REFPAC 200 (Imerys, France) were dry mixed in the planetary mixer for 1 min and after water addition, another 6 min. All castables were cast under mechanical vibration for 2 min, cured at room temperature in humidity chamber for 24h in moulds and after demoulding left for 72h in the open air. After curing, castable samples were dried at 110°C for 24h and sintered at 1600°C with 2h dwell.

Table I. Model castable formulations

Name	Cas_12S78_6CMA	Cas_12S78_6CAC	Cas_6S78_12CMA	Cas_0S_18CMA	Cas_16S78_2CAC
Raw materials [mass %]					
TA 6-3 mm	23	23	23	23	23
TA 3-1 mm	10	10	10	10	10
TA 1-0.5 mm	19	19	19	19	19
TA 0.5-0.0 mm	24	24	24	23	24
Calcined Alumina	2	2	2	2	2
Bimodal Reactive Alumina	3	3	3	4	3
Spinel AR 90 < 45 µm	0	0	0	0	0
Spinel AR 78 < 45 µm	5	5	0	0	7
Spinel AR 78 < 20 µm	7	7	6	0	9
CMA Cement	6	0	12	18	0
CAC Cement	0	6	0	0	2
Disp. Additive	1	1	1	1	1
Water	4,4	4,4	4,4	4,4	4,4
Variation in the MA and CaO content					
CaO	0,6	1,8	1,2	1,8	0,6
MA	12	12	6	0	16
MA (CMA)	4,2	0	8,4	12,6	0
Total MA	16,2	12	14,4	12,6	16

2.2 Methods

2.2.1 Damping and Young's modulus determination with the Impulse Excitation Technique (IET)

Damping and Young's modulus temperature dependency was characterized non-destructively via Impulse Excitation Technique (IET) from flexural vibrations with the use of the HT RFDA system provided by IMCE, Belgium. All measurements were performed during heating – cooling up to 1500°C cycle with the rate of 5 K/min and 1 h dwell at the maximum temperature.

2.2.2 Hot Modulus of Rupture (HMOR)

HMOR tests were conducted at defined temperatures upon heating and cooling cycle between 25°C - 1500°C with 1h dwell the maximum temperature and 5K/min heating – cooling rate.

2.2.3 Thermal shock resistance testing with High Temperature Thermal Shock Furnace

Thermal shock tests were performed with a custom-made High Temperature Thermal Shock Furnace **(GHI, RWTH Aachen University)** by repeated sample transportation between two high temperature chambers. Each thermal cycle consist of two thermal shocks; descendant by the transportation form hot chamber to cold chamber and ascendant when returning to hot chamber. Schematic illustration of the High Temperature Thermal Shock Furnace is presented in **Fig.1**.

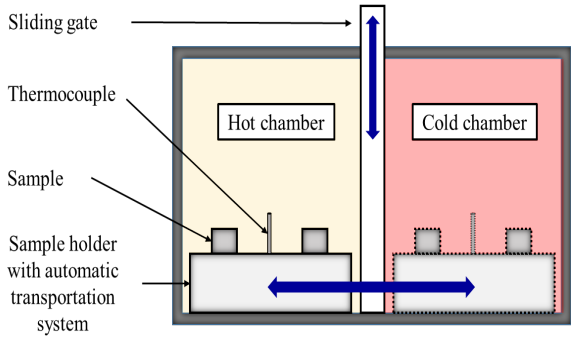

Fig. 1 Schematic of the HT Thermal Shock Furnace

Thermal shock testing of alumina-spinel brick was realized in order to investigate the influence of the relaxation peak on the thermal shock performance. Alumina-spinel brick samples were tested under two different thermal shock programs varied by different temperature in cold chamber and therefore different ΔT. Detailed information about two thermal shock programs is summarized in **Table II.**

Table II. Thermal shock conditions in case of alumina-spinel brick.

No	Heating rate [K/min]	Temperature in hot chamber [°C]	Dwell time in hot chamber [min]	Temperature in cold chamber [°C]	Dwell time in cold chamber [min]	Cooling rate [K/min]
1	5	1500	30	**1250**	120	5
2	5	1500	30	**1075**	120	5

Thermal shock resistance of five alumina-spinel castables was investigated with two different methods. In order to examine the possible correlation between high damping capacity and thermal shock resistance, a thermal shock test was realized with High Temperature Thermal Shock Furnace by repeated sample transportation between two high temperature chambers (900°C and 1500°C) with 1,5h of dwell in each chamber. A comparative study was conducted with the application of standard air quenching technique involving samples introduction to the furnace at 950°C (hot shock) followed by rapid cooling under compressed air (cold shock).

The evolution of the progressive thermal shock damage was realized nondestructive via Young's modulus determination.

2.2.4 Creep In Compression (CIC)

Creep in compression of five alumina-spinel castables was determined with the RUL/CIC apparatus (NETZSCH) using a cylindrical test piece (diameter and height ~ 50 mm) with a co-axial bore of 12.5 mm.

3. RESULTS AND DISCUSSION

3.1 Damping properties of alumina-spinel refractories

Damping spectrum of alumina-spinel brick (**Fig. 2**) is characterized by the presence of two perfectly defined damping peaks, denoted P_I and P_{II} superimposed on wide exponentially increasing high-temperature damping background. The two damping peaks P_I and P_{II} develop both during heating and cooling stage, with strong hysteretic effect for P_I, therefore peaks observed during heating and cooling stage are respectively marked with $_h$ and $_c$.

Halbwachs [7] at all were the first to report a perfectly defined internal friction peak in the non-stoichiometric $(A1_20_3)_{3.5}MgO$ spinel of an exceptional strength. Further investigations confirmed the responsible mechanisms associated with stress-induced reorientation of Mg2+—V'' pairs.

The existence of a second peak in internal friction spectrum of alumina-rich spinel has not been reported in literature. Therefore, it is assumed that the spinel itself is not responsible for the development of the second damping peak (P_{II}). A possible explanation should be rather sought in alumina-spinel interaction at high temperature, which leads to the development of microstresses.

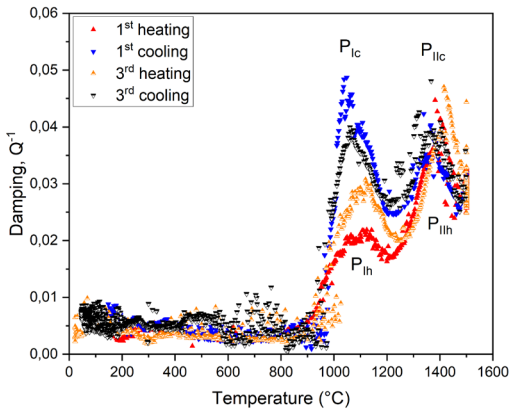

Fig. 2 Damping temperature dependency of alumina-spinel brick.

The development of exponentially increasing damping background at high-temperature is quite common for most of the materials. Increasing damping background is typically assumed to be related

with grain boundary sliding.

The average damping capacity of alumina-spinel castables during 1h dwell at 1500°C is summarized in **Table III**. High temperature damping properties of alumina-spinel castables seems to be influenced by the total spinel content and submicron spinel addition (via CMA addition). Damping capacity at high temperature can be related apart from grain boundary sliding, to the diffusional processes and microstructural development at the $MgAl_2O_4$/ Al_2O_3 interface. Such a hypothesis would explain the increasing damping tendency with the increasing number of $MgAl_2O_4$/Al_2O_3 interfaces.

Table III. The avaerage damping capacity of alumina-spinel castables at 1500°C.

Q^{-1} x 10^{-3} [-]	Cas_12S78 _6CMA	Cas_12S78 _6CAC	Cas_6S78 _12CMA	Cas_0S_ 18CMA	Cas_16S78 _2CAC
$Q^{-1}_{1500°C}$	37	25	29	50	39

3.2 Damping, Young's Modulus and HMOR

Fig. 3 displays variation of the E/E0 ratio during two subsequent heating-cooling cycles combined with the damping spectrum of alumina-spinel brick.

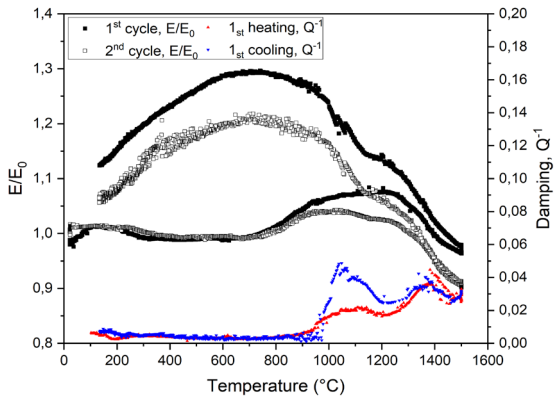

Fig. 3 Variation of E/E_0 and Q^{-1} as a function of temperature.

After a slight initial decrease up to around 400°C, the Young's modulus is stable up to 650°C, where a positive Young's modulus anomaly starts to develop. The Young's modulus increase takes place in a broad temperature range starting from around 800°C. Beyond 1250°C significant decrease is observed up to the maximum test temperature of 1500°C. During cooling significant stepwise increase of Young's modulus value takes place up to around 700°C. Similar Young's modus anomalies were observed [8] in the case of pure plasma sprayed polycrystalline nonstoichiometric spinel $(Al_2O_3)_3MgO$, where the first positive anomaly with the increase of about 7 % at 700°C was attributed to the exsolution reaction and precipitation of intermediate metastable phases. The second strong positive Young's modulus anomaly, ascribed to the precipitation of α-Al_2O_3 from spinel structure, was revealed to develop between 1000 and 1300°C.

Fig. 4 shows correlation between damping characteristic and obtained HMOR results.

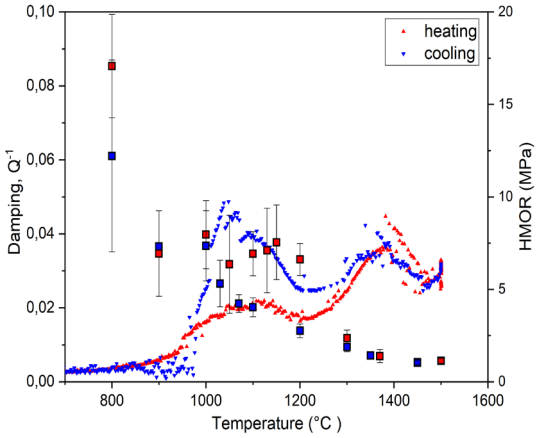

Fig. 4 Correlation between HMOR and damping properties of alumina spine brick.

As expected, with increasing temperature the HMOR values significantly decrease with is usually attributed to the weakening of grain boundaries. Nevertheless, it is seen that in the temperature range of the first damping peak, the bending strength achieve some plateau up to 1200°C. Above this temperature, a further significant drop of

HMOR value takes place. The presence of such a plateau may be similarly connected with a microstructural strengthening due to the exsolution reaction and precipitation phenomena in non-stoichiometric spinel crystals. It is worth pointing out that HMOR values during subsequent cooling stage are significantly lower than for the heating stage, which does not coincide with the observations based on temperature-dependent Young's modulus results. A significant increase in Young's modulus value during cooling combined with slight decrease in HMOR properties could be explained by the complex precipitation sequence and formation of various precipitate substructures, which exhibit distinct influence on mechanical properties.

3.3 Damping and Thermal Shock Resistance

Young's modulus value evolution as a function of progressively applied thermal shock cycles with two different ΔT applied in the case of alumina-spinel brick is presented in **Fig. 5.**

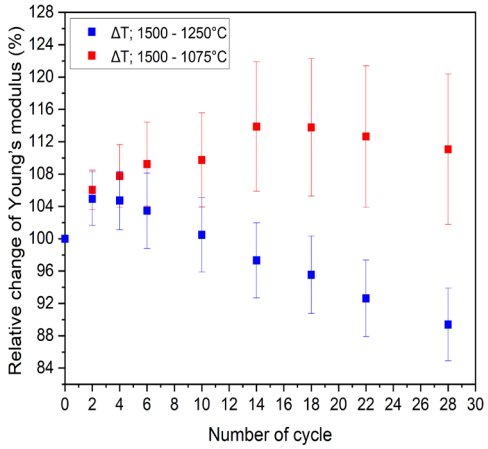

Fig. 5 Relative change of Young's modulus value due to progressive thermal cycling.

The Young's modulus evolution due to thermal cycling according to two different programs exhibit distinct behavior. Successive thermal cycling between 1500°C and 1250°C is associated with Young's modulus depletion starting from the fourth cycle. Whereas in the second case the thermal cycling between 1500°C – 1075°C leads to gradual increase of Young's modulus value, despite higher ΔT applied. The superior behavior of alumina-spinel brick under more severe thermal shock conditions may originate from two distinct microstructural phenomena; additional energy dissipation mechanism during crack propagation and precipitation which could strengthen the microstructure and heal the cracks.

Thermal shock results obtained for alumina-spinel castables determined with the use of standard air quenching procedure are presented in **Fig. 6** and with the use of the HT Thermal Shock Furnace in **Fig. 7**.

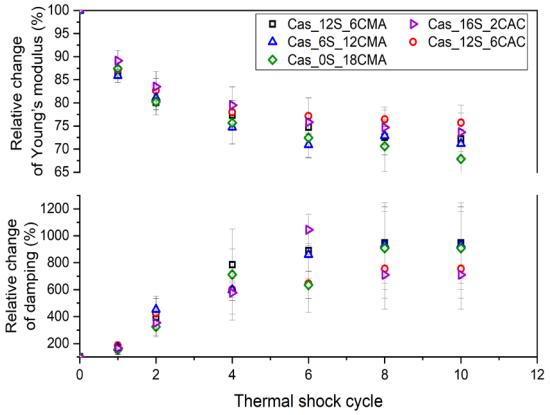

Fig. 6 Thermal shock resistance of alumina-spinel castables under standard air quenching conditions.

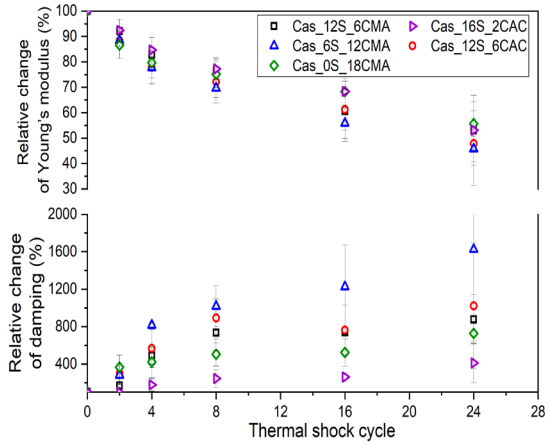

Fig. 7 Thermal shock resistance of alumina-spinel castables under HT Thermal Shock conditions

Thermal shock results obtained by standard air quenching technique revealed superior resistance of castables bonded with CAC over castables bonded with CMA cement, which is in line with the literature data [9] reporting that binders containing submicron spinel particles could be responsible for the development of high strength and high Young's and thus reduced thermal shock resistance due to increased sintering reactivity of the matrix. In contradiction to the results obtained by standard thermal shock procedure are results obtained by HT Thermal Shock Furnace. Thermal cycling at high temperature revealed superior thermal cycling resistance of castables bonded with a high amount of CMA cement: Cas_0S_18CMA and higher spinel addition: Cas_12S_6CMA, Cas_16S_2CAC. As authors previously stated [10], high temperature damping properties should influence material performance under thermal cycling conditions. The superior behavior of alumina-spinel castables exhibiting higher damping capacity may originate from their higher ability to relax thermal stresses induced by extensive thermal cycling and their enhanced ability to dissipate energy at the crack tip which promotes crack propagation blunting [11].

3.4 High-temperature damping and creep

Fig. 7 compares the creep behavior of five alumina-spinel castables at 1500°C.

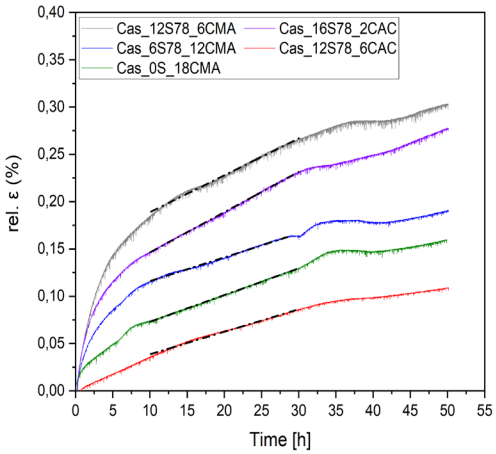

Fig. 7 Creep test results of alumina-spinel castables at 1500°C

As can be seen, lower creep resistance was obtained for castables containing a higher amount of spinel, followed by castables bonded with CMA cement, ending with superior creep resistance of castables containing the lowest amount of spinel, the highest of CaO and bonded with CAC cement. Reported here results are in tune with the literature data [12] stating improved creep resistance with reduced spinel content in alumina-spinel fired bricks. Increased creep resistance of castables containing a higher amount of spinel may be linked with dynamic precipitation of α-Al_2O_3 under the application of external stresses, which has been demonstrated to promote plastic deformation [13]. The superior creep resistance of castables Cas_12S78_6CAC and Cas_0S_18CMA could be additionally linked with higher CaO content resulting in CA_6 formation at high temperatures. Platelet-like grains of CA_6 has been proven [14] to provide increased creep resistance, which was attributed to the grain bridging mechanism.

In order to highlight a relatively good correlation between the creep deformation

and damping properties, damping evolution as a function of time at 1500°C is presented in **Fig. 8**

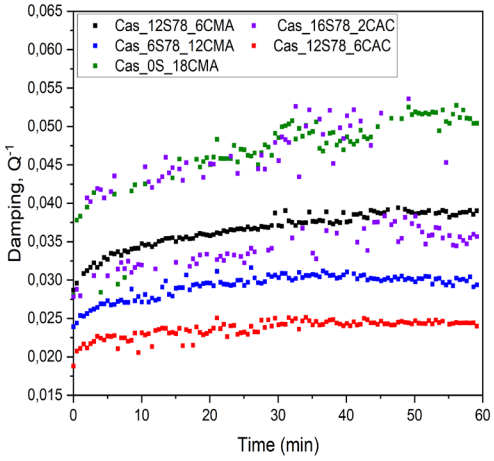

Fig. 8 Time-dependent damping spectrum of alumina-spinel castables at 1500°C

Presented time-dependent damping spectra reveal lower and rather constant damping capacity of castables Cas_12S78_6CAC and Cas_6S78_12CMA. Higher and increasing over time damping characteristic is observed for castables with higher spinel content and maximum value of CMA addition. It is noteworthy to note similarities between presented creep and time-dependent damping results. As expected, the order of the constable's creep resistance corresponds nearly to the order of time-dependent damping capacity, with the only one exception for castable bonded with CMA in the amount of 18 %. The superior creep resistance of the high-damping castable could be linked with the unique combination of the microstructure containing high amount of interlocking and strengthening CA_6 pallets and a high amount of fine-grained submicron spinel providing high damping capacity.

4. CONCLUSIONS

Alumina-spinel refractories that contain alumina-rich spinel develop typical damping peaks which seem to originate from the subsequent structural transformations. Castables with a higher spinel content and higher amount of submicron spinel grains develop better high temperature damping capabilities, which is probably related to the ongoing process at the alumina spinel interface. The Young's modulus, HMOR, creep and results were found in good agreement with the damping properties. High Temperature Thermal Shock Furnace was employed to investigate the influence of stress relaxation phenomena on thermal shock resistance of alumina-spinel refractories. It has been shown that improved thermal cycling resistance could originate from enhanced stress relaxation ability and/or precipitation phenomena. CMA bonded castables seems to be good candidates for high-damping refractories, with an increased thermal shock resistance.

REFERENCES

[1] M. Matsuzawa, S. Horibe, J. Sakai, "Anelasticity and Strength in Zirconia Ceramics", Key Eng. Mater., 280–283, pp 967–972, (20070.

[2] M. Matsuzawa, M. Abe, S. Horibe, "Strain rate dependence of tensile behavior and environmental effect in zirconia ceramics", ISIJ Int., 43 [4] pp 555–563 (2003).

[3] R. Schaller, J.J. Ammann, A. Kulik, C. Bonjour, W. Benoit, "Internal friction spectrum of WC-Co composite alloys", J. Phys., 46 [12] pp 387-390 (1985).

[4] C. Mayencourt, R. Schaller, "A High-Damping Magnesium Matrix to Limit Fatigue in Composite", J. Reinf. Plast. Compos., 18 [18] pp 1677–1688 (1999).

[5] E. Carreno-Morelli, S. Urreta, L. Gabella, R. Schaller, "Thermal Stress Relaxation in Al-Al_2O_3 (f) Composites During Thermal Cycling", Journal de Physique IV Proceedings, 6 pp 735-738 (1996).

[6] K. Ishizaki, K.Niihara, M. Isotani M, R.G. Ford, “Grain Boundary Controlled Properties of Fine Ceramics”, ed. Springer, pp 77-87 (1992).
[7] M. Halbwachs, P. Mazot, J. Woirgard, “Anelastic relaxation phenomena in plasma-sprayed $(Al_2O_3)_3MgO$ spinel with reference to diffusion process”, Phys. status solidi, 76 [1] pp 157–164 (1983).
[8] D. Fargeot, C. Gault, F. Platon, P. Boch “Elastic and anelastic effects associated with precipitation phenomena in non stoichiometric spinels”, Journal de Physique Colloques, 42 [C5] pp C5-899-C5-904 (1981).
[9] C. Wöhrmeyer, S. Gao, M. Szepizdyn, F. Simonin, “Optimization of Thermal Shock Resistance Alumina-Spinel Castables”, 64 pp 182–187 (2015).
[10] I. Kieliba, T. Tonnesen, R. Telle, M. Huger, E. Guéguen, “Alumina-Spinel Castables under Thermal Cycling Conditions - In Situ Characterisation”, Proceeding Unitecr 2019, pp 912–915, (2019).
[11] R. Schaller, “Mechanical spectroscopy of the high-temperature brittle-to-ductile transition in ceramics and cermets”, J. Alloys Compd., 310 [1–2] pp 7–15, (2000).
[12] I.S. Kainarskii, I.G. Orlova, R.E. Vol'fson, “Creep in granular corundum-spinel refractories”, Refractories, 10 pp 751–758 (1969).
[13] P. C. Panda, R. Raj, P. E. D. Morgan, “Superplastic Deformation in Fine-Grained MgO $2Al_2O_3$ Spinel”, J. Am. Ceram. Soc., 68 10, pp 522–529, (1985).
[14] M. A. L. Braulio, V. C. Pandolfelli, “Tailoring the Microstructure of Cement-Bonded Alumina–Magnesia Refractory Castables”, J. Am. Ceram. Soc., 93 [10] pp 2981–2985 (2010).

Acknowledgments: this work was supported by the funding scheme of the European Commission, Marie Skłodowska-Curie Actions Innovative Training Networks in the frame of the project ATHOR - Advanced THermomechanical multiscale modelling of Refractory linings 764987 Grant.
The authors are also grateful to the JECS Trust for funding the visit of Ilona Kieliba to IRCER - University of Limoges (Contract No. 2018169).